

22

One hadron inclusive production

22.1 Process and fragmentation functions

We shall be concerned here with the one hadron production inclusive process:

$$e^+e^- \rightarrow \gamma^*(s) \rightarrow H + X, \quad (22.1)$$

which is the twin in the timelike region of the leptonproduction discussed previously on the target \bar{H} :

$$\gamma^*(-s) + \bar{H} \rightarrow X. \quad (22.2)$$

In the centre of mass of γ^* :

$$q = (\sqrt{s}, \mathbf{0}), \quad (22.3)$$

the kinematics of the process can be described by the momentum p of the hadron H and the fraction of beam energy $z\sqrt{s}/2$, where $0 \leq z \leq 1$:

$$p = (z\sqrt{s}/2, \mathbf{p}). \quad (22.4)$$

By formal analogy with leptonproduction, one can introduce the structure functions $\bar{F}_{1,2}^H(z, Q^2)$, such that the angular differential cross-section reads:

$$\frac{d\sigma}{dzd\cos\theta} = \frac{3}{4}\tilde{\sigma}^{(0)}_z \left[2\bar{F}_1(z, s) + \frac{z}{2}\sin^2\theta\bar{F}_2(z, s) \right], \quad (22.5)$$

where in the naïve parton with spin 1/2 quarks:

$$\tilde{\sigma}^{(0)} = \frac{4\pi\alpha^2}{3s}. \quad (22.6)$$

Alternatively, one can introduce the transverse and longitudinal structure functions:

$$\begin{aligned} \bar{F}_T(z, Q^2) &= 2\bar{F}_1(z, Q^2) \\ \bar{F}_L(z, Q^2) &= 2\bar{F}_1(z, Q^2) + z\bar{F}_2(z, Q^2), \end{aligned} \quad (22.7)$$

with which one can express the differential cross-section:

$$\frac{d\sigma}{dz} = \tilde{\sigma}^{(0)}_z \left[\bar{F}_T(z, s) + \frac{1}{2}\bar{F}_L(z, s) \right], \quad (22.8)$$

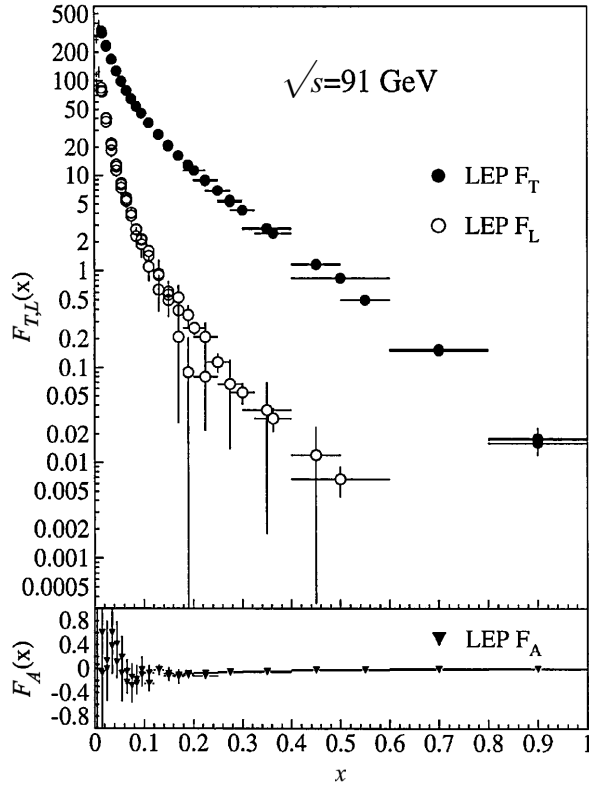


Fig. 22.1. Transverse $\bar{F}_T \equiv F_T$ and longitudinal $\bar{F}_L \equiv F_L$ fragmentation functions versus x at $\sqrt{Q} = 91$ GeV. F_A is a parity-violating contribution coming from the interference between the vector and axial-vector contributions.

where in the naïve parton with spin 1/2 quarks:

$$\begin{aligned} \bar{F}_L(z, s) &= 0 \\ \bar{F}_T(z, s) &= 3 \sum_i Q_i^2 [D_{0q_i}^H(z) + D_{0\bar{q}_i}^H(z)] . \end{aligned} \tag{22.9}$$

$D_{0q_i}^H$ is the fragmentation or decay function, which is the number of density of H in the jet of parton p .

The data of these functions compiled by [16] are given in Fig. 22.1.

22.2 Inclusive density, correlations and hadron multiplicity

As in all inclusive processes, one can define the inclusive total cross-section:

$$\sigma_{\text{tot}} = \sum_H \sigma_H , \tag{22.10}$$

as the sum of all exclusive channels production of H particles. The one particle inclusive cross-section density is:

$$\rho(p) = \frac{1}{\sigma_{\text{tot}}} \frac{p^0 d\sigma}{d^3 p}, \quad (22.11)$$

for a particle of momentum p . Similarly for two particles 1 and 2, the inclusive density is defined as:

$$\rho(p_1, p_2) = \frac{1}{\sigma_{\text{tot}}} \frac{p_1^0 p_2^0 d\sigma}{d^3 p_1 d^3 p_2}, \quad (22.12)$$

and one can define their correlations:

$$C(p_1, p_2) = \rho(p_1, p_2) - \rho(p_1)\rho(p_2). \quad (22.13)$$

The *average hadron multiplicity* for one inclusive particle are defined as:

$$\langle n_H \rangle = \int \frac{d^3 p}{p^0} \rho(p), \quad (22.14)$$

and for two particles:

$$\langle n_1 n_2 \rangle = \int \frac{d^3 p_1 d^3 p_2}{p_1^0 p_2^0} \rho(p_1, p_2). \quad (22.15)$$

In the same way, one can also define the third isospin components for the hadron H :

$$I_3 = \frac{1}{\sigma} \sum_H \int d^3 p I_3^H \frac{d\sigma_H}{d^3 p}. \quad (22.16)$$

22.3 Parton model and QCD description

To the leading order approximation, one has for each parton p :

$$\begin{aligned} \sum_H \int_0^1 dz I_3^H D_{0p}^H(z) &= I_3^p \\ \sum_H \int_0^1 dz D_{0p}^H(z) &= 1, \end{aligned} \quad (22.17)$$

where the first equation reflects the non-singlet charge conservation sum rule, while the second is the momentum conservation in the jet of parton p . The parton model description of a one hadron inclusive production is shown in Fig. 22.2, where the photon produces a hard parton p with four momentum k and with an energy fraction y of the beam energy:

$$k = (y\sqrt{s}/2, \mathbf{k}), \quad (22.18)$$

such that, independently of other partons, the produced parton fragments into hadrons. One expects that no hard interactions can take place between produced partons because their separation in rapidity is too wide at higher energies. In the limit of massless partons and

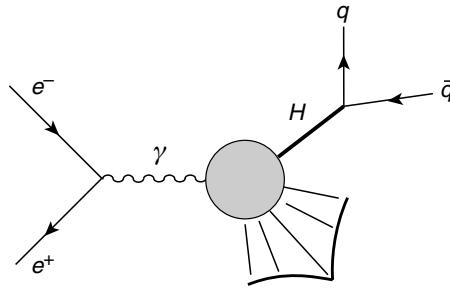


Fig. 22.2. $e^+e^- \rightarrow \gamma^* \rightarrow H + \text{all}$ in the parton model.

negligible intrinsic transverse momentum of the fragments, one has the relation between the hadron and parent parton:

$$p = (z/y)k . \tag{22.19}$$

The cross-section for producing a hadron H with fraction z of the beam energy is obtained as a convolution of the cross-section for producing a parton with energy fraction y times the density of a hadrons H in the parton p with the fraction z/y of the proton momentum:

$$z\bar{\mathcal{F}}_a^H(z, s) = \frac{1}{\bar{\sigma}^{(0)}} \int_z^1 \frac{dy}{y} \sum_i \sigma_a^{\gamma^* \rightarrow p_i}(y, s) D_{0p_i}^H(z/y) , \tag{22.20}$$

where:

$$\bar{\mathcal{F}}_a^H = (2\bar{F}_1^H, -z\bar{F}_2^H) . \tag{22.21}$$

In the case of the naïve parton model, the cross-section reads:

$$\sigma^{\gamma^* \rightarrow q} = 3 \sum_i Q_i^2 \delta(1 - z) . \tag{22.22}$$

One can easily see that the inclusive quark production cross-section to order α_s is:

$$\begin{aligned} \sigma^{\gamma^* \rightarrow q}(x_q < 1) &= \frac{C_F}{2} \left(\frac{\alpha_s}{\pi}\right) \int_{1-x_q}^1 dx_{\bar{q}} \frac{x_q^2 + x_{\bar{q}}^2}{(1-x_q)(1-x_{\bar{q}})} = \frac{C_F}{2} \left(\frac{\alpha_s}{\pi}\right) \frac{1+x_q^2}{1-x_q} t + \dots \\ &= \frac{1}{2} \left(\frac{\alpha_s}{\pi}\right) P_{qq}(x_q)t + \dots \end{aligned} \tag{22.23}$$

where the log-divergence of the integral at $x_{\bar{q}} = 1$ has been re-interpreted as a factor $t \equiv (1/2) \ln(Q^2/v^2)$.

In the same way, the cross-section production of a gluon is:

$$\begin{aligned} \sigma^{\gamma^* \rightarrow g}(x_g) &= \frac{C_F}{2} \left(\frac{\alpha_s}{\pi}\right) \int_{1-x_g}^1 dx_q \frac{x_q^2 + (2-x_{\bar{q}}-x_q)^2}{(1-x_q)(x_q+x_g-1)} \\ &= 2\frac{C_F}{2} \left(\frac{\alpha_s}{\pi}\right) \frac{1+(1-x_g)^2}{x_g} t + \dots = 2C_F \left(\frac{\alpha_s}{\pi}\right) P_{gq}(x_g)t + \dots . \end{aligned} \tag{22.24}$$

where the factor 2 indicates that the gluons can be emitted either by quark or by antiquarks. Therefore, one can deduce:

$$z\bar{\mathcal{F}}_a^H(z, s) = \frac{1}{\bar{\sigma}^{(0)}} 3Q^2 \int_z^1 \frac{dy}{y} \left\{ \left[\delta(1-y) + \left(\frac{\alpha_s}{\pi}\right) \left(tP_{qq}(y) + \frac{1}{2}\bar{f}_q^a(y) \right) \right] \right. \\ \left. \times \left[D_{0q}^H(z/y) + D_{0\bar{q}}^H(z/y) \right] + \left(\frac{\alpha_s}{\pi}\right) \left(2tP_{qg}(y) + \frac{1}{2}\bar{f}_g^a(y) \right) D_{0g}(z/y) \right\}, \tag{22.25}$$

where the sum over flavours is understood. As in the case of electroproduction for the structure functions, the fragmentation functions obey similar Altarelli–Parisi evolution equations. To order α_s , it reads:

$$\frac{\partial}{\partial t} D_{q_i}(z, t) = \left(\frac{\alpha_s}{\pi}\right) [P_{qq} \otimes D_{q_i} + P_{gq} \otimes D_g] \\ \frac{\partial}{\partial t} D_g(z, t) = \left(\frac{\alpha_s}{\pi}\right) \left[P_{qg} \otimes \sum_i (D_{q_i} + D_{\bar{q}_i}) + P_{gg} \otimes D_g \right], \tag{22.26}$$

where the only difference with electroproduction is the transposition $P_{qg} \leftrightarrow P_{gq}$. In terms of the singlet and non-singlet fragmentation functions:

$$D_{NS} = D_{q_i} - D_{q_j} \\ D_S = \sum_i (D_{q_i} + D_{\bar{q}_i}), \tag{22.27}$$

the evolution equations read:

$$\frac{\partial}{\partial t} D_S(z, t) = \left(\frac{\alpha_s}{\pi}\right) [P_{qq} \otimes D_S + 2n_f P_{gq} \otimes D_g] \\ \frac{\partial}{\partial t} D_g(z, t) = \left(\frac{\alpha_s}{\pi}\right) [P_{qg} \otimes D_S + P_{gg} \otimes D_g]. \tag{22.28}$$

Factorization of the perturbative (hard gluon radiation) and non-perturbative (hadronization) regime at a scale μ_f in the time-like region has been proved by many authors (see, however, the notion of fracture functions introduced in [268]). In this case, the inclusive cross-section of the process can be expressed as:

$$\frac{d\sigma}{dx}(e^+e^- \rightarrow H + X) = \sum_i \int_z^1 \frac{dy}{y} C_i(y, \mu^2, \mu_f^2) D_i^H(z/y, \mu_f^2), \tag{22.29}$$

where C_i are Wilson coefficients calculable perturbatively and correspond to the cross-section for the creation of a hard parton i and a momentum fraction y of the beam energy; D_i is the fragmentation function (density of a hadron H in a parton i with fraction z/y of the parton momentum). The coefficient functions vanish to lowest order for gluons and are known to higher orders. However, the previous factorization assumption may not work, and it can be more appropriate to introduce the notion of *fracture functions*. The phenomenology of fragmentation functions has been discussed in the literature using different Monte-Carlo

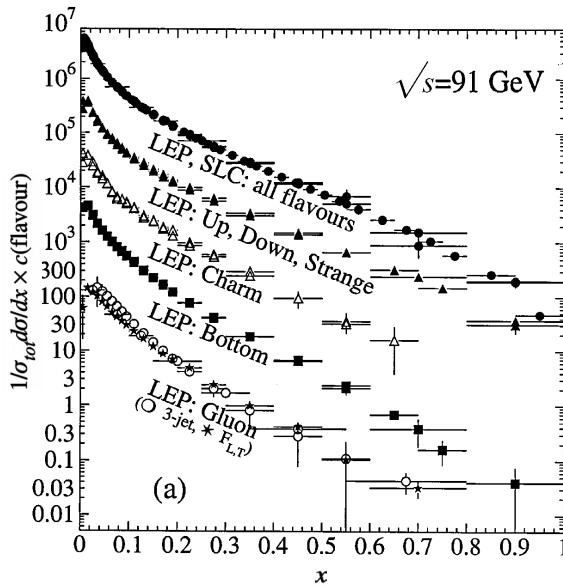


Fig. 22.3. Charged-particle and flavour-dependent e^+e^- fragmentation functions versus x at $\sqrt{Q} = 91$ GeV. The data are shown for the inclusive, light (u, d, s), c and b quarks, and the gluon. The distributions were scaled by $c(\text{flavour}) = 10^n$, where n ranges from $n = 0$ (gluon) and $n = 4$ (all flavours).

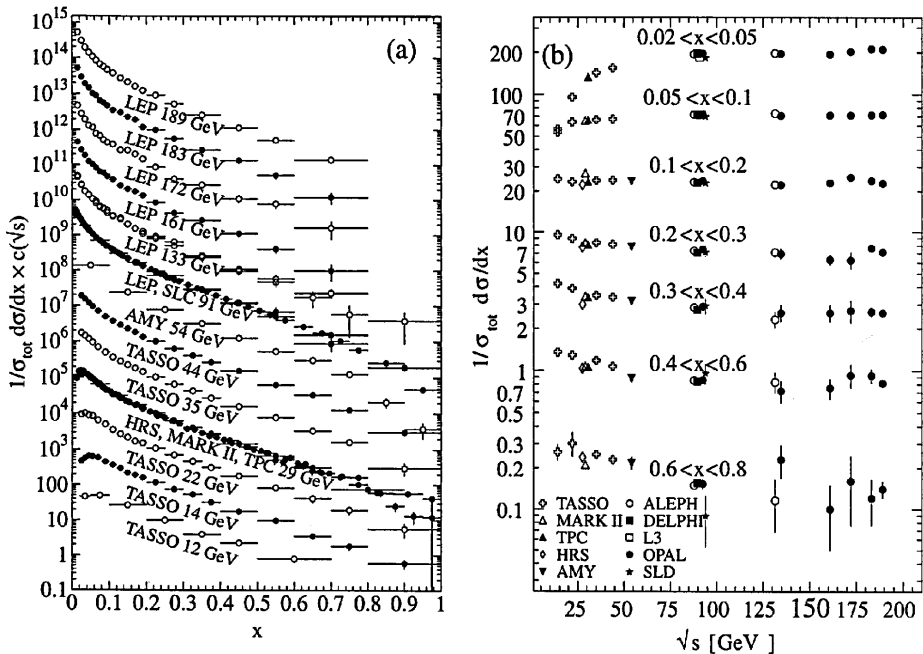


Fig. 22.4. All charged-particle e^+e^- fragmentation functions (a) for different c.m. energies \sqrt{s} , versus x and (b) for different x versus \sqrt{s} . The data are shown for the inclusive, light (u, d, s), c and b quarks, and the gluon. For plotting (a), the distributions were scaled by $c(\sqrt{s}) = 10^i$, where i ranges from $i = 0$ ($\sqrt{s} = 12$ GeV) to $i = 12$ ($\sqrt{s} = 189$ GeV).

simulation programs (see e.g. [277]). Detailed analyses of the charged hadron fragmentation functions have been performed by different LEP groups using data samples at PETRA, PEP and LEP energies from c.m. energy in the range from 14 to 92 GeV. We show the data in Figs. 22.3 and 22.4.

These analyses have been used for extracting α_s and some QCD power-like corrections. Combined ALEPH [278] and DELPHI [279] results give:

$$\alpha_s(M_{Z^0}) = 0.125^{+0.006}_{-0.007} (\text{exp}) \pm 0.009 (\text{theo}), \quad (22.30)$$

where the theoretical uncertainties are mainly due to the scale variations.